SLEEPJ, 2021, 1–12

doi: 10.1093/sleep/zsaa202
Advance Access Publication Date: 26 September 2020
Original Article

ORIGINAL ARTICLE

Identifying neuroanatomical signatures in insomnia and migraine comorbidity

Kun-Hsien Chou[1,2], Pei-Lin Lee[2], Chih-Sung Liang[3,], Jiunn-Tay Lee[4,5], Hung-Wen Kao[6], Chia-Lin Tsai[4], Guan-Yu Lin[4], Yu-Kai Lin[4,5], Ching-Po Lin[1,2,7,] and Fu-Chi Yang[4,*,]

[1]Brain Research Center, National Yang-Ming University, Taipei, Taiwan, [2]Institute of Neuroscience, National Yang-Ming University, Taipei, Taiwan, [3]Department of Psychiatry, Beitou Branch, Tri-Service General Hospital, National Defense Medical Center, Taipei, Taiwan, [4]Department of Neurology, Tri-Service General Hospital, National Defense Medical Center, Taipei, Taiwan, [5]Graduate Institute of Medical Sciences, National Defense Medical Center, Taipei, Taiwan, [6]Department of Radiology, Tri-Service General Hospital, National Defense Medical Center, Taipei, Taiwan and [7]Department of Biomedical Imaging and Radiological Sciences, National Yang-Ming University, Taipei, Taiwan

*Corresponding author. Fu-Chi Yang, Department of Neurology, Tri-Service General Hospital, National Defense Medical Center, No. 325, Section 2, Cheng-Kung Road, Neihu 114, Taipei, Taiwan R.O.C. Email: fuji-yang@yahoo.com.tw.

Abstract

Study Objectives: While insomnia and migraine are often comorbid, the shared and distinct neuroanatomical substrates underlying these disorders and the brain structures associated with the comorbidity are unknown. We aimed to identify patterns of neuroanatomical substrate alterations associated with migraine and insomnia comorbidity.

Methods: High-resolution T1-weighted images were acquired from subjects with insomnia, migraine, and comorbid migraine and insomnia, respectively, and healthy controls (HC). Direct group comparisons with HC followed by conjunction analyses identified shared regional gray matter volume (GMV) alterations between the disorders. To further examine large-scale anatomical network changes, a seed-based structural covariance network (SCN) analysis was applied. Conjunction analyses also identified common SCN alterations in two disease groups, and we further evaluated these shared regional and global neuroanatomical signatures in the comorbid group.

Results: Compared with controls, patients with migraine and insomnia showed GMV changes in the cerebellum and the lingual, precentral, and postcentral gyri (PCG). The bilateral PCG were common GMV alteration sites in both groups, with decreased structural covariance integrity observed in the cerebellum. In patients with comorbid migraine and insomnia, shared regional GMV and global SCN changes were consistently observed. The GMV of the right PCG also correlated with sleep quality in these patients.

Conclusion: These findings highlight the specific role of the PCG in the shared pathophysiology of insomnia and migraine from a regional and global brain network perspective. These multilevel neuroanatomical changes could be used as potential image markers to decipher the comorbidity of the two disorders.

Statement of Significance

Insomnia and migraine are often comorbid; however, shared and distinct neuroanatomical substrates underlying these disorders are unknown. Using T1 voxel-based morphometry and seed-based structural covariance network analyses, this study identified multilevel neuroanatomical substrates associated with insomnia, migraine, and comorbid migraine and insomnia. This study identified the specific role of the postcentral gyri in the patients with comorbid migraine and insomnia from the regional and global brain network perspectives. Our findings suggest that multilevel neuroanatomical changes could be potential image markers in patients with comorbid insomnia and migraine. The findings provide insights into the neuroanatomical signatures related to the pathophysiology of comorbidity of the two common disorders.

Key words: insomnia; migraine; comorbidity; network; gray matter volume

Submitted: 28 April, 2020; **Revised:** 26 August, 2020

Introduction

Insomnia is a prevalent sleep disorder worldwide, which affects approximately 10% of the population [1]. Symptoms of insomnia disorder include difficulties falling asleep, staying asleep, and experiencing refreshing sleep [1]. Insomnia is also associated with reduced quality of life, cognitive and affective impairments, work disabilities, traffic accidents, and a marked increase in health care burden [2]. Despite the great socioeconomic impact of insomnia, its pathophysiology is still poorly understood. Insomnia is suggested to be closely associated with various neurological disorders, especially migraine [3].

Migraine is a primary headache disorder affecting 10%–20% of the general population, predominantly women, characterized by recurrent lateralized, intense headaches, associated with nausea, vomiting, sound sensitivity, and light sensitivity [4]. Poor sleep quality is common, affecting 30%–50% of migraineurs. Additionally, sleep disruptions, especially insomnia, can trigger migraine attacks that may have been avoided with sufficient restful sleep, and people with chronic migraine are prone to headache recurrences [5]. Although pathophysiological mechanisms have been proposed linking insomnia and migraine, including disturbances of the serotonin descending pain inhibitory system [6], and the hypothalamic orexinergic system [7], the neuroanatomical mechanisms underlying their comorbidity are lacking.

In migraine, neuroanatomical alterations have been reported in many brain regions, including the insula, the motor/premotor, prefrontal, cingulate, posterior parietal, orbitofrontal, and somatosensory cortices, and the caudate nucleus [8, 9]. The structural abnormalities in the brains of patients with insomnia remain controversial and diverse; structural neuroimaging studies have disclosed anatomical alterations in the hippocampus [10], anterior cingulate cortex [11], and orbitofrontal cortex [12]. Accumulating evidence also suggests structural and functional alterations in a broad network including pain processing and sensorimotor networks [13, 14]. Collectively, alterations in widespread anatomical areas have been reported in both insomnia and migraine disorders. However, it is largely unknown if shared neuroanatomical regions are associated with the comorbidity of insomnia and migraine disorders.

To identify brain regions associated with disease effect using regional morphological features, large-scale structural covariance network (SCN) analysis was recently proposed as a candidate approach to characterize inter-regional coordination between distinct anatomical brain areas [15, 16]. Furthermore, recent research suggested that inter-regional coordination profiles between the cerebellum and remote cortical regions are associated with the clinical outcome of patients with migraine [17]. Therefore, comparison of regional morphological brain features and global large-scale SCN analysis could provide two different but complementary approaches for investigating anatomical brain changes and further help elucidate the pathophysiology of comorbidity between the two disorders.

We applied T1 voxel-based morphometry (VBM) and seed-based SCN analyses to data from patients with migraine, insomnia, and comorbid conditions to identify regional and global anatomical substrates associated with the comorbidity. First, direct VBM group comparisons with healthy controls (HC) were followed by conjunction analyses to identify regions of shared gray matter volume (GMV) alterations in both disorders. Second, to investigate associated large-scale structural networks changes at the identified comorbidity sites, seed-based SCN analyses were applied to the shared GMV change regions; network-level conjunction analyses were employed to identify common large-scale structural network alterations in both diseases. Third, an additional group with comorbid migraine and insomnia was used to evaluate the replicability of these shared multilevel neuroanatomical signatures, and exploratory association and classification analyses were applied to evaluate their potential clinical significance.

Methods

Participants

The study protocol was approved by the institutional review board of Tri-Service General Hospital (TSGH). All participants provided informed written consent before enrollment. Participants were recruited consecutively from the Headache Clinic at the Neurology Department of TSGH: 40 participants diagnosed with migraine (80.0% female; migraine with aura, n = 6; migraine without aura, n = 34), 22 with primary insomnia (68.2% female), 27 with comorbid migraine and primary insomnia (85.2% female; migraine with aura, n = 4; migraine without aura, n = 23), and 27 HC (77.8% female) with no history of neurological or psychiatric disease.

Diagnosis of migraine adhered to the third edition of the International Classification of Headache Disorders (ICHD-III) [18]. Secondary or other concomitant primary headache disorders were excluded. Furthermore, we documented the clinical characteristics of all participants diagnosed with migraine, including migraine duration, frequency, aura symptoms, family history, and headache intensity. All migraine patients were migraine-free for at least 3 days prior to examination and were followed-up 3 days after the scanning to ensure that they had remained migraine-free to avoid any possible interference from headache pain on the imaging results.

In this study, primary insomnia was diagnosed according to DSM-V criteria [19] as assessed by a structured clinical interview. A brief self-reported questionnaire of the Insomnia Severity Index (ISI) was implemented for all participants to evaluate their perception of insomnia severity [20]. The ISI is composed of seven items that evaluate aspects of insomnia symptoms; each ISI item is rated on a scale of 0–4. The total ISI score is divided into four categories: 0–7, no clinically significant insomnia; 8–14, sub-threshold insomnia; 15–21, moderate insomnia; and 22–28, severe insomnia. The ISI was not used for diagnosis of primary insomnia. Medical and psychiatric disorders were evaluated via structured diagnostic interview, physical examination, blood tests (blood cell count, thyroid, renal, and hepatic function), and urine drug testing (for benzodiazepines, opiates, barbiturates, amphetamines, and cannabis). Patients with secondary insomnia were excluded during the recruitment if they had the following: other sleep or psychiatric disorders (e.g. hypersomnia or parasomnia); insomnia associated with specific causes (e.g. drugs, alcohol, or mental illness; history of heart disease, stroke, nephritis, or psychiatric diseases); or abnormalities in brain structure such as brain tumors or hematoma. No patient was treated with migraine preventive medication, dopaminergic agents, antidepressants, neuroleptics, or hypnotics.

Demographic and clinical data including the patient's sex, age, insomnia duration; sleep quality (assessed with the Pittsburgh Sleep Quality Index [PSQI] [21], Beck Depression Inventory [BDI] score [22], and the Hospital Anxiety and Depression Scale [HADS] score [23]) were also documented. No acute migraine attacks occurred during the scanning sessions.

The HC group comprised volunteers without insomnia or migraine, matched for age, sex, and handedness. HC were recruited through community advertisements and hospital patient pools. Exclusion criteria for HC included a family history of insomnia or migraine, a prior diagnosis of a primary or secondary headache disorder, and any chronic pain condition.

MRI data acquisition

All participants underwent identical MRI scan sessions on a 3.0T Discovery MR750 scanner (General Electric Healthcare, Milwaukee, WI) with an eight-channel head array coil. Three-dimensional axial T1-weighted scans were collected using an inversion recovery prepared fast spoiled gradient recalled sequence with the following parameters: repetition time/echo time/inversion time = 10.17/4.16/450 msec, flip angle = 12°, number of excitations = 1, field of view = 256 × 256 mm^2, matrix size = 256 × 256, 172 slices, and voxel size = 1 × 1 × 1 mm^3. All images were acquired parallel to the anterior commissure-posterior commissure line without inter-slice gap and interpolation. An experienced neuroradiologist visually examined all raw MRI scans to exclude organic brain disorders. No participant was excluded for brain abnormalities. Before subsequent image processing, we reoriented all images to have an approximate point of origin using a center-of-mass approach.

Voxel-wise GMV calculations using VBM

Voxel-wise GMV maps were extracted from T1-weighted images using a VBM approach [24]. A VBM pipeline was implemented using functionalities provided by the Statistical Parametric Mapping software (SPM12, version 7487, Wellcome Institute of Neurology, University College London, UK, http://www.fil.ion.ucl.ac.uk/spm/) and the Computational Anatomy Toolbox (CAT12, version 1363, http://www. neuro.uni-jena.de/cat/) in a MATLAB environment (version R2015a; Mathworks, Natick, MA). All T1-weighted images were corrected for bias-field homogeneities, classified into gray matter (GM), white matter (WM), and cerebrospinal fluid (CSF), followed by affine aligning to the Montreal Neurological Institute (MNI) template space using the CAT12 toolbox. The weighted overall image quality rating (IQR), which combines measurements of noise, bias, and resolution of the original T1-weighted image, was calculated for the initial quality assurance test. Scans with an IQR below 75% were excluded from the subsequent analyses. Next, the Diffeomorphic Anatomical Registration Through Exponentiated Lie (DARTEL) algebra toolbox was used to create a study-specific template, via iterative nonlinear warping of the affine-aligned GM and WM segments of all participants, and further normalizing individual tissue segments to the constructed template [25]. The DARTEL deformation field was then corrected to generate the MNI space-modulated GM segments and further resampled to the final spatial resolution of 1.5 mm^3. Once the above steps were completed, the CAT12 "Check Sample Homogeneity" function, together with careful visual inspection, was used to assess the data quality of the modulated GM segments. No participant was identified as an outlier. Finally, modulated GMV maps were smoothed with an isotropic Gaussian filter (full-width-half-maximum = 8 mm) and voxels with a GM probability lower than 0.2 were excluded to minimize partial volume effects on different tissue borders. Global tissue volume and total intracranial volume (TIV = GM + WM + CSF volumes) were estimated for each participant in native T1 space using the "Estimate TIV and global tissue volumes" module (part of CAT12 toolbox). To further minimize any potential confounding effects including variations in age, sex, global brain size, or degree of depression, we used a general linear model with age, sex, TIV, and HADS score as nuisance variables to obtain the voxel-wise residualized modulated GMV map for each individual. These individual residualized modulated GMV maps served as inputs for the following voxel-wise statistical analyses.

Statistical analyses

Demographic and clinical characteristics, global tissue volume, and image quality

Statistical analyses of all non-voxel-wise data were conducted using IBM SPSS Statistics (version 22, IBM Corp., Armonk, NY). Analyses of variance (ANOVA; age and IQR), chi-square tests (sex and aura status), and analyses of covariances (global tissue volume and clinical characteristics) were used to identify statistical differences between the respective study groups. Two-tailed p values <0.05 were considered statistically significant in all analyses.

Analyses of voxel-wise image-based investigations

SPM12 with appropriate statistical models was used for the following voxel-wise statistical analyses. For all analyses, a cluster-extent approach was used for correcting multiple comparisons. The updated "3dFWHMx" and "3dClustSim" programs, which are implemented in the Analysis of Functional Neuroimages software (AFNI, version 19.1.18; 10,000 Monte Carlo simulations with explicit GM mask; https://afni.nimh.nih.gov/), determined the minimum cluster size for maintaining a family-wise error (FWE) rate-corrected p value <0.05. Using an initial voxel-level p value <0.005, results indicated that clusters larger than 208 voxels were considered significant at a corrected cluster level. For transparency and reusability of statistical results, we uploaded all unthresholded voxel-wise statistical maps to the NeuroVault website via the following permanent link (https://neurovault.org/collections/5796/). Details about the statistical models are indicated below.

Identification of shared and distinct GMV alterations in patients with migraine or insomnia and HC

To determine the shared GMV changes between HC and patients with migraine or insomnia, a two-step statistical approach was applied [26]. First, a one-factor three-level (migraine, insomnia, and HC) ANOVA was conducted to identify the regional GMV discrepancies between the patient groups and HC (migraine vs HC/insomnia vs HC). These two statistical contrasts were further used for the conjunction test to identify shared anatomical changes in the two disease groups by searching the intersection of the voxel-wise FWE-corrected

p-maps. In addition, we used the statistical contrast of the direct group comparison between the two disease groups to identify anatomical regions with distinct GMV changes (migraine vs insomnia).

Shared large-scale SCN changes in patients with migraine and insomnia

Using the anatomical regions that were identified in the previous conjunction analysis as predefined seed regions of interests (ROIs), we first used two separate multiple regression models (bilateral postcentral gyrus [PCG]) to map typical whole-brain large-scale SCNs of the mean GMV of the predefined seed ROIs within HC [27, 28]. To further explore the potential disease-specific effects of the corresponded large-scale SCN, a group main effect term, a mean seed ROI volume main effect term, and a group × mean seed ROI volume interaction term were contained in a separate general model for each predefined ROI. By testing the statistical significance of the interaction term at each voxel (migraine vs HC/insomnia vs HC), this statistical design enabled us to identify regional differences in the structural covariance integrity of the predefined ROIs between HC and the two disease groups [16, 29]. Finally, we applied the same conjunction analysis to the corresponding statistical contrasts to identify the shared SCN changes in the two disease groups. Finally, we applied the same conjunction analysis to the corresponding statistical contrasts to identify the shared SCN changes in the two disease groups.

Replication analysis of shared regional and global neuroanatomical signatures in the comorbid migraine/insomnia group

To test whether the same regional GMV and global SCN changes were consistently found in the comorbid patient group, the following analytical pipeline was applied. First, for regional GMV changes, a voxel-wise two-sample *t*-test was used to identify GMV changes between HC and the comorbid patient group. Next, we overlapped these thresholded voxel-wise statistical results with previous results of the regional GMV conjunction analysis in the standard MNI space, to assess the spatial relationship between the two analyses. The same analytical flow with appropriate statistical models (multiple regression analysis to test SCN changes in the comorbidity group and HC, followed by spatial overlap with the results of the previous conjunction analysis of SCN changes in patients with migraine and insomnia) was also applied to replicate the findings of the SCN analysis.

Evaluation of the global spatial similarity of neuroanatomical changes between study groups

We used unthresholded *t*-statistic maps with a spatial spin permutation test as a complementary approach to evaluate the spatial similarity of neuroanatomical changes between disease cohorts and the comorbid group. In brief, we first computed Pearson correlations between the unthresholded *t*-statistic maps of the selected contrast (migraine vs HC and comorbid group vs HC/insomnia vs HC and comorbid group vs HC) for each hemisphere. Next, we determined the significance of spatial correspondence using a spatial spin permutation test approach with 1,000 permutations. This approach generates a null distribution by comparing a target unthresholded *t*-statistic map to a permutated map, which is created by randomly rotating the spherical projections of the cortical surface while preserving the spatial relationships within the data [30]. The relevant code for conducting the spin permutation test can be found using the following link (https://github.com/rudyvdbrink/surface_projection).

Clinical significance of the regional GMV and global structural covariance changes

To explore the potential clinical implications of the shared regional and global neuroanatomical signatures in patients with comorbid migraine and insomnia, the regional GMV (extracted and averaged from the cluster of the previous voxel-wise conjunction analysis) and the integrity of structural covariance were estimated for each individual. As the changes in the integrity of structural covariance were identified by group-level statistical results, we further applied the recent proposed approach to obtain a single measure that quantified the integrity of the inter-regional structural covariance for each individual [31]. These regional and global measurements were then used for the following two distinct statistical analyses to explore the potential clinical significance. First, we conducted an exploratory Pearson's correlation analysis to investigate the association between neuroanatomical signatures and clinical evaluations including migraine duration, migraine frequency, headache intensity, insomnia duration, and ISI and PSQI scores (uncorrected p value <0.05). Second, three logistic regression models (Model 1: regional GMV only, Model 2: global structural covariance integrity only, Model 3: regional GMV combined with global structural covariance integrity) were constructed to assess the diagnostic capacity of the regional and global neuroanatomical signatures in differentiating patients with comorbidity from HC. A receiver-operating characteristic (ROC) curve analysis and an area under the curve (AUC) analysis with a 1,000-times bootstrapping resampling scheme were employed to evaluate the efficacy of the three logistic regression models (80% of subjects were randomly extracted for each resample). An ANOVA test was then conducted to determine if the three models were statistically significantly different.

Results

Demographic and clinical characteristics of the participants

The major clinical characteristics of the participants are presented in Table 1. In this study, we enrolled 27 HC (age range = 21–62 years), 40 patients with migraine (age range = 20–57 years), 22 patients with primary insomnia (age range = 22–57 years), and 27 patients with comorbid migraine and primary insomnia (age range = 17–56 years). Four groups were matched for age, sex, and handedness. Scores for insomnia, anxiety, depression, and sleep quality assessments worsened in patients with insomnia and comorbid migraine and insomnia (p value <0.05). There were no significant differences in total GMV, WM volume, CSF volume, or TIV among the four groups. None of the conventional T1 structural images from any participant showed morphological abnormalities or image artifacts.

Regional GMV changes between patients with migraine or insomnia and HC

Migraine versus HC

GMV differences in patients with migraine relative to HC are shown in Table 2 and Figure 1, A (FWE-corrected p value <0.05). Relative to HC, regions of smaller GMV were observed in the

Table 1. Demographics and clinical characteristics of study participants

Demographic variables	HC (n = 27)	MIG (n = 40)	INSO (n = 22)	MIG with INSO (n = 27)	P value
Age (years)	41.3 ± 10.1	39.2 ± 10.5	40.2 ± 11.7	40.6 ± 11.3	0.894*
Sex (male/female)	6/21	8/32	7/15	4/23	0.540†
GMV	600.7 ± 50.3	595.9 ± 53.7	582.1 ± 35.6	590.2 ± 53.8	0.694‡
WMV	496.5 ± 68.2	487.0 ± 49.5	479.7 ± 56.6	496.8 ± 54.1	0.421‡
CSFV	345.4 ± 68.4	343.8 ± 64.4	322.9 ± 46.7	337.5 ± 45.9	0.801‡
TIV	1,443.6 ± 166.7	1,427.8 ± 137.9	1,385.7 ± 114.8	1,425.5 ± 127.7	0.073§
IQR (%)	84.2 ± 0.6	84.1 ± 0.8	84.2 ± 0.7	84.5 ± 0.6	0.229*
Aura/no aura	–	6/34	–	4/23	0.983‖
Migraine duration (years)	–	14.7 ± 10.2	–	14.1 ± 9.7	0.825¶
Migraine frequency (days/month)	–	9.9 ± 6.5	–	12.6 ± 9.1	0.133¶
Insomnia duration (month)	–	–	24.1 ± 28.2	5.7 ± 6.4	0.067¶
ISI total score (0–28)	4.9 ± 4.6	5.8 ± 4.4	17.0 ± 1.1	15.8 ± 6.4	<0.001§
PSQI total score (0–21)	5.7 ± 3.2	6.1 ± 3.9	10.3 ± 2.8	11.3 ± 3.4	<0.001§
HADS score (0–42)	9.4 ± 5.3	11.4 ± 6.9	13.8 ± 8.1	16.8 ± 7.7	0.005§
BDI score (0–63)	6.2 ± 6.0	7.8 ± 6.5	14.0 ± 9.5	14.3 ± 9.6	0.001§

All patients with migraine or insomnia, HC, or patients with comorbid migraine and insomnia were right-handed. BDI, Beck Depression Inventory score; CSFV, cerebrospinal fluid volume; GMV, gray matter volume; HADS, Hospital Anxiety and Depression Scale score; HC, healthy controls; INSO, insomnia; IQR, image quality rating; ISI, Insomnia Severity Index; MIG, migraine; PSQI, Pittsburgh Sleep Quality Index; TIV, total intracranial volume; WMV, white matter volume.*Four-group analysis of variance test.
†Four-group chi-square test.
‡Four-group analysis of covariance adjusted for age, sex, and TIV.
§Four-group analysis of covariance adjusted for age and sex.
‖Two-group chi-square test.
¶Two-group analysis of covariance adjusted for age and sex.

Table 2. Anatomical regions with significant GMV changes in migraine patients, insomnia patients, patients with comorbid migraine and insomnia, and HC

MNI coordinate				Residualized GMV (mean ± *SD*)			
x, y, z	Cluster size	Maximum t-value	Anatomical region	HC	MIG	INSO	MIGwINSO
HC > MIG							
42, −23, 59	447	3.97	Rt. postcentral gyrus	0.358 ± 0.034	0.326 ± 0.034	0.323 ± 0.037	0.336 ± 0.034
−29, −68, −17	325	3.57	Lt. cerebellum VI	0.552 ± 0.055	0.511 ± 0.038	0.523 ± 0.054	0.530 ± 0.051
−41, −15, 42	559	3.54	Lt. precentral gyrus	0.311 ± 0.036	0.280 ± 0.041	0.280 ± 0.024	0.290 ± 0.037
HC < MIG							
−13, −49, 62	265	3.52	Lt. postcentral gyrus	0.295 ± 0.026	0.326 ± 0.036	0.297 ± 0.044	0.304 ± 0.035
HC > INSO							
42, −21, 62	1,217	3.87	Rt. precentral gyrus	0.337 ± 0.030	0.311 ± 0.028	0.300 ± 0.025	0.313 ± 0.027
−44, −13, 47	418	3.58	Lt. precentral gyrus	0.338 ± 0.040	0.306 ± 0.043	0.301 ± 0.025	0.315 ± 0.044
2, −75, 5	313	3.21	Rt. lingual gyrus	0.364 ± 0.041	0.343 ± 0.040	0.329 ± 0.028	0.355 ± 0.048
HC > MIG with INSO							
32, −29, 53	404	3.79	Rt. postcentral gyrus	0.306 ± 0.037	0.281 ± 0.037	0.276 ± 0.049	0.273 ± 0.031
29, −39, −53	395	3.73	Rt. cerebellum VIIIb	0.358 ± 0.039	0.338 ± 0.043	0.348 ± 0.041	0.321 ± 0.038
−18, −75, 36	318	3.36	Lt. cuneal cortex	0.358 ± 0.057	0.335 ± 0.050	0.350 ± 0.052	0.313 ± 0.045
HC < MIG with INSO							
39, 24, −30	248	3.77	Rt. temporal pole	0.308 ± 0.043	0.334 ± 0.046	0.316 ± 0.055	0.345 ± 0.034
−45, −48, −32	233	3.53	Lt. cerebellum crus I	0.347 ± 0.037	0.374 ± 0.059	0.380 ± 0.041	0.384 ± 0.044

Peak of group differences in residualized GMV, with a threshold of FWE-corrected p value < 0.05. GMV, gray matter volume; HC, healthy controls; INSO, insomnia; Lt, left; MIG, migraine; MNI, Montreal Neurological Institute; Rt, right; *SD*, standard deviation.

right PCG, left precentral gyrus, and cerebellum of patients with migraine, while regions of greater GMV in patients were observed in the left PCG.

Insomnia versus HC

Relative to HC, regions of smaller GMV were observed in the bilateral precentral gyri and the right lingual gyrus in patients with insomnia. No anatomical area with increased GMV was found in patients with insomnia (Table 2 and Figure 1, B; FWE-corrected p value <0.05).

Migraine versus insomnia

No significant GMV differences were observed in patients with insomnia relative to patients with migraine (FWE-corrected p value <0.05).

GMV alterations common to migraine and insomnia (shared GMV alterations)

Conjunction analysis showed GMV decreases in the bilateral PCG in both disorders (Figure 1, C), while no region showed shared GMV increases.

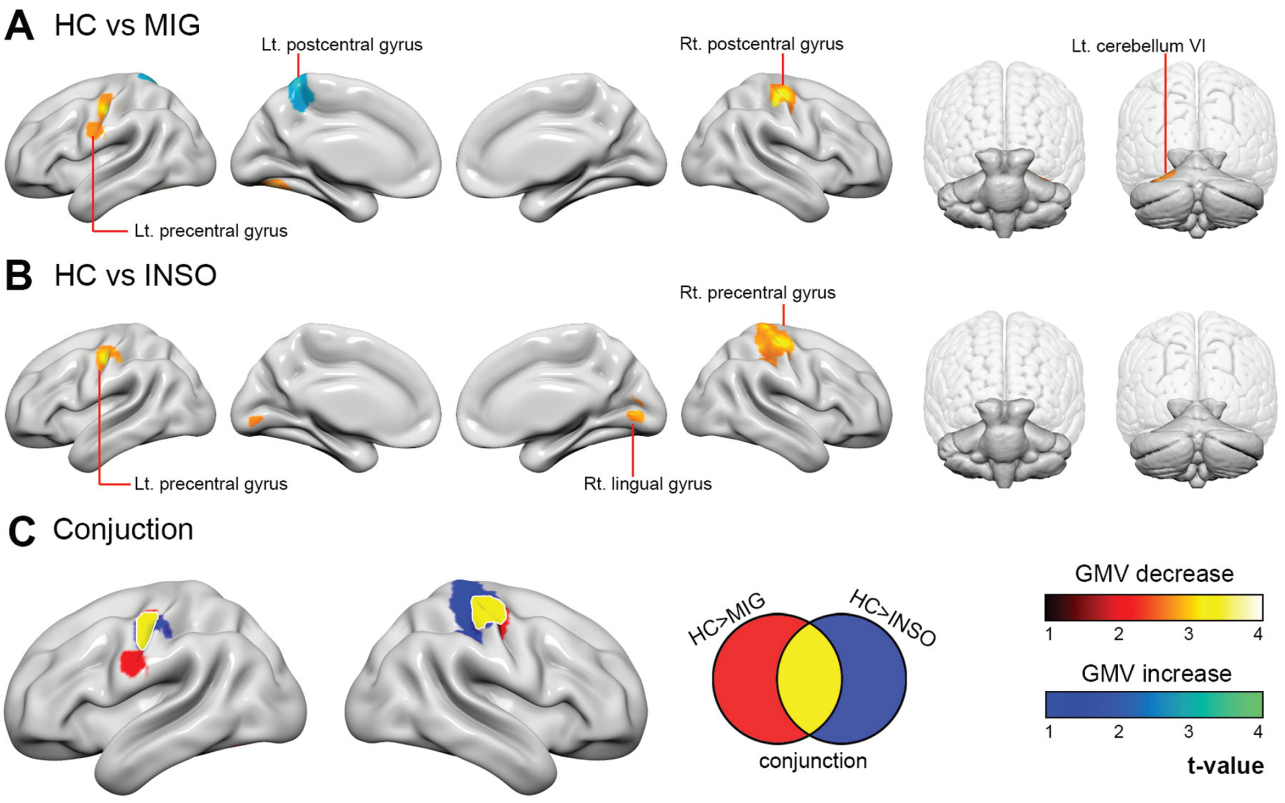

Figure 1. (A) GMV differences between patients with migraine and HC as revealed by VBM. Cold (blue) colors indicate significantly greater regional GMV in patients with migraine; warm (red) colors indicate significantly lower regional GMV. (B) GMV differences between patients with insomnia and HC. Warm (red) colors indicate significantly lower regional GMV in patients with insomnia. (C) Conjunction analyses showing the PCG as the common GMV alteration site in both patient groups (yellow). GMV, gray matter volume; HC, healthy controls; INSO, insomnia; Lt, left; MIG, migraine; PCG, postcentral gyrus; Rt, right; VBM, voxel-based morphometry.

Differences in the integrity of bilateral PCG SCN between patients with migraine or insomnia and HC

SCN changes of the right PCG seed in migraine and insomnia

In HC, the right PCG showed strong structural covariance with the bilateral prefrontal cortex as well as with the bilateral somatosensory cortex (SSC) and cerebellum (Figure 2, A). Relative to HC, in patients, regions of decreased integrity of structural covariance were observed in the bilateral cerebellum, while regions of increased integrity of structural covariance were observed in the left middle temporal gyrus (Table 3 and Figure 2, B; FWE-corrected p value <0.05).

Relative to HC, regions of decreased integrity of structural covariance were observed in the bilateral cerebellum, left frontal pole, PCG, and right supplementary motor cortex (Table 3 and Figure 2, C; FWE-corrected p value <0.05).

SCN changes of the left PCG seed in migraine and insomnia

In HC, similar to the pattern of whole-brain structural covariance of the right PCG, the left PCG also demonstrated structural covariance with the bilateral prefrontal cortex as well as with the bilateral SSC and cerebellum (data not shown, available in the NeuroVault website). Relative to HC, regions of decreased integrity of structural covariance were observed in the left frontal orbital cortex, superior temporal gyrus, right cerebellum, and bilateral pallidum in patients with migraine (Table 3, FWE-corrected p value <0.05).

No areas showed structural covariance patterns of left PCG differences in patients with insomnia relative to HC.

SCN alterations of the right PCG seed common to migraine and insomnia

The conjunction analysis revealed that in both disorders, the right PCG showed decreased integrity of structural covariance with the right cerebellum compared with the controls (Figure 2, C), while no region showed shared increased integrity of structural covariance with the right PCG.

Patients with comorbid migraine and insomnia versus HC (shared patterns of multilevel neuroanatomical signature replicated in the comorbidity group).

Relative to HC, regions of decreased GMV were observed in the left cuneal cortex, the right PCG, and the right cerebellum, while regions of increased GMV were observed in the right temporal pole and the left cerebellum for comorbid patients. Specifically, altered GMV was consistently found in the right PCG in patients with comorbid migraine and insomnia relative to HC (Table 2 and Figure 3, A, FWE-corrected p value <0.05).

Relative to HC, decreased integrity of structural covariance of the left PCG was observed in the right cerebellum in patients, while increased integrity of structural covariance of the left PCG was observed in the right central opercular cortex and the left occipital pole (Table 3, FWE-corrected p value <0.05). Relative to HC, decreased integrity of structural covariance of the right PCG was observed in the left frontal pole, right temporal, and frontal poles, and the cerebellum of patients, while increased integrity of structural covariance of the right PCG was observed in the left cerebellum. Specifically, decreased integrity of structural covariance of the right PCG was consistently found in the right

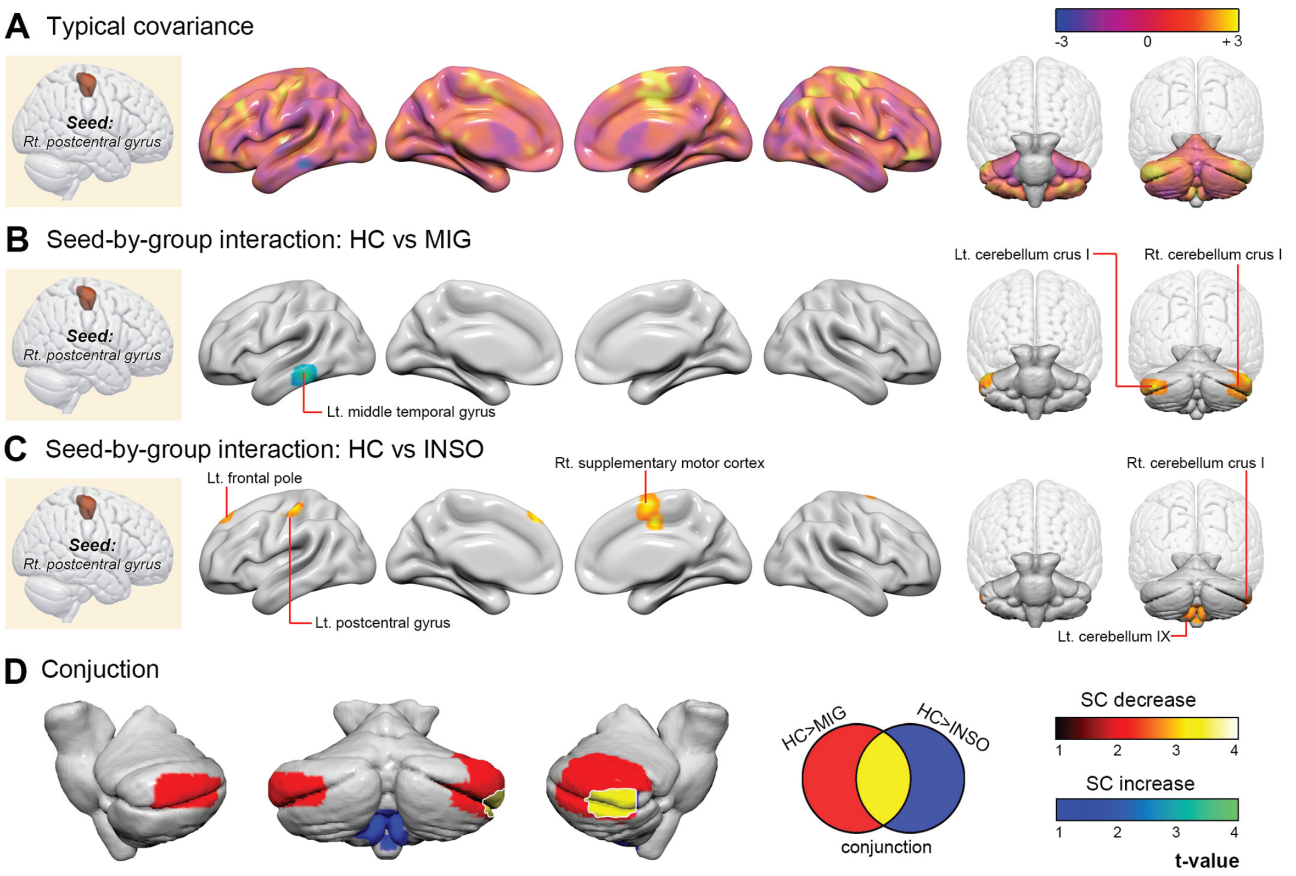

Figure 2. (A) Spatial distribution of the structural covariance pattern from the right PCG was mapped in the HC group. (B) SC pattern differences of the right PCG between patients with migraine and HC. Cold (blue) colors indicate significantly greater SC integrity of the right PCG in patients with migraine; warm (red) colors indicate significantly lower SC integrity of the right PCG. (C) SC pattern differences of the right PCG between patients with insomnia and HC. Warm (red) colors indicate significantly lower SC integrity of the right PCG in patients with insomnia. (D) Conjunction analyses showing SC alterations of the right PCG common to both patient groups, located in the right cerebellum. HC, healthy controls; INSO, insomnia; Lt, left; MIG, migraine; PCG, postcentral gyrus; Rt, right; SC, structural covariance.

cerebellum in patients with comorbid migraine and insomnia, relative to HC (Figure 3, B).

Global patterns of the neuroanatomical changes between patients with migraine, insomnia, and comorbid migraine and insomnia.

Using spatial spin permutation test, we identified statistically significant spatial correspondence of the HC-vs-MIG with INSO and HC-vs-MIG *t*-statistic maps (left hemisphere: $r = 0.581$, p value < 0.001; right hemisphere: $r = 0.664$, p value < 0.001) and HC-vs-INSO t-statistic maps (left hemisphere: $r = 0.496$, p value < 0.001; right hemisphere: $r = 0.507$, p value < 0.001), respectively (Supplementary Figure S1).

these two distinct signatures with three logistic regression models and corresponding ROC analyses. The ROC analyses demonstrate the classification performance of the three distinct models (differentiating patients with comorbid migraine and insomnia from HC): GMV of the right PCG (Model 1), integrity of structural covariance between right PCG and right cerebellum (Model 2), and a combined regional GMV and global structural covariance integrity index (Model 3). Using a bootstrap resampling scheme, the AUC results indicate that Model 3 (mean AUC = 0.809, CI = 0.807–0.811) significantly outperformed Model 2 (mean AUC = 0.742, CI = 0.739–0.744) and Model 1 (mean AUC = 0.660, CI = 0.658–0.663) (p value < 0.001, Figure 4).

Potential clinical significance of regional GMV and global SCN changes in the comorbidity group

Our exploratory analysis revealed that among patients with comorbid migraine and insomnia, sleep quality (assessed using the PSQI score) correlated negatively with the regional GMV of the right PCG ($r = -0.408$, uncorrected p value = 0.038). None of the areas with significant changes in SC of the right PCG demonstrated a statistically significant association with the clinical variables.

To further assess the diagnostic ability of the identified regional and global neuroanatomical signatures, we validated

Potential effects of the degree of depression and anxiety in the neuroanatomical alterations

To gain more insight into the effects of the participant's emotional characteristics on neuroanatomical alterations, we also performed an additional Pearson correlation analysis to evaluate the potential associations between HADS, residual GMV of the right PCG and SC integrity of the PCG-cerebellum. There were no statistically significant associations between HADS and residual GMV of the right PCG ($r = -0.011$, p value = 0.910) or SC integrity of PCG-cerebellum ($r = 0.054$, p value = 0.567). We further added BDI scores as covariates and performed the same voxel-wise

Table 3. Anatomical regions with significant altered structural covariance of bilateral PCG migraine patients, insomnia patients, patients with comorbid migraine and insomnia, and HC

MNI coordinate				Integrity of structural covariance			
x, y, z	Cluster size	Maximum *t*-value	Anatomical region	HC	MIG	INSO	MIGwINSO
Seed: Rt. PCG							
HC > MIG							
45, −62, −29	2,546	4.04	Rt. cerebellum crus I	0.613*	−0.325*	0.121	−0.177
−42, −83, −38	761	3.52	Lt. cerebellum crus I	0.583*	−0.170	0.206	−0.181
HC < MIG							
−57, −33, −12	339	4.48	Lt. middle temporal gyrus	−0.762**	0.356*	0.040	0.136
HC > INSO							
3, −2, 54	447	3.92	Rt. supplementary motor cortex	0.709**	0.251	−0.203	0.061
−13, 43, 52	216	3.81	Lt. frontal pole†	0.594*	0.331*	−0.341	0.156
−1, −59, −62	422	3.42	Lt. cerebellum IX	0.461*	0.144	−0.396	0.016
−48, −25, 59	260	3.38	Lt. postcentral gyrus	0.495*	0.543**	−0.430*	0.238
51, −58, −43	261	3.06	Rt. cerebellum crus I	0.599*	−0.271	−0.178	−0.271
HC > MIG with INSO							
−47, 54, −8	438	4.59	Lt. frontal pole	0.485*	0.324*	0.226	−0.482*
−44, −81, −39	639	4.20	Lt. cerebellum crus I	0.604*	−0.128	0.149	−0.329
29, 6, −24	225	4.11	Rt. temporal pole†	0.443*	0.271	0.261	−0.547*
44, −66, −44	945	3.98	Rt. cerebellum crus II	0.577*	−0.270	−0.020	−0.339
55, 41, −6	237	3.15	Rt. frontal pole	0.712**	0.251	0.202	−0.073
HC < MIG with INSO							
−27, −74, −59	212	3.65	Lt. cerebellum VIIb†	−0.306	−0.135	−0.454*	0.536*
Seed: Lt. PCG							
HC < MIG							
11, 7, −1	607	4.37	Rt. pallidum	−0.686**	0.305	−0.089	−0.096
−9, 21, −29	409	4.29	Lt. frontal orbital cortex	−0.463*	0.349*	0.162	−0.038
−9, 22, −3	858	3.80	Lt. pallidum	−0.659**	0.338*	−0.162	−0.093
−69, −14, −3	288	3.39	Lt. superior temporal gyrus	−0.399*	0.396*	−0.219	0.257
36, −39, −36	515	3.34	Rt. cerebellum VI	−0.491*	0.326*	0.169	0.002
HC > MIG with INSO							
18, −47, −50	266	3.70	Rt. cerebellum VIIIb	0.477*	−0.004	0.483*	−0.403*
HC < MIG with INSO							
53, 1, 0	296	3.89	Rt. central opercular cortex	−0.270	0.194	0.034	−0.710**
−16, −92, 38	430	3.70	Lt. occipital pole	−0.425*	0.036	−0.152	0.513*

Peak of group differences in integrity of structural covariance of bilateral PCG, with a threshold of FWE-corrected p value < 0.05. FWE, family-wise error; HC, healthy controls; INSO, insomnia; Lt, left; MIG, migraine; MNI, Montreal Neurological Institute; PCG, postcentral gyrus; ROI, regions of interest; Rt, right.

*$p < 0.05$.

**$p < 0.001$.

†The region would not pass the statistical criteria which consider multiple comparison correction for the multiple ROI seeds (FWE-corrected p value < 0.025).

statistical analyses. The results of the voxel-wise GMV comparisons and seed-based SCN analysis remained similar after controlling for these two scales, respectively (Supplementary Figure S2 for regional GMV comparisons and Supplementary Figure S3 for seed-based SCN comparisons, FWE-corrected p value < 0.05). The following Pearson correlation analyses also demonstrated that there were no statistically significant associations between BDI and residual GMV of the right PCG (r = −0.098, p value = 0.296) or SC integrity of the PCG-cerebellum (r = −0.048, p value = 0.614).

Discussion

In the present study, patients with migraine or insomnia both show several areas with GMV alterations relative to HC, in the bilateral PCG, bilateral precentral gyri, right lingual gyri, and left cerebellum. Our conjunction analysis demonstrates that the two disorders share similar patterns of GMV changes in the bilateral PCG. Further seed-based SCN analyses of the shared GMV change regions, followed by conjunction analyses, identified common structural covariance alterations of the right PCG in both disease groups, located in the right cerebellum. Moreover, alterations in GMV and structural covariance integrity of the right PCG were consistently found in patients with comorbid migraine and insomnia. Finally, the GMV of the right PCG demonstrated an association with sleep quality, and the combined regional GMV and structural covariance integrity of the PCG showed good discriminative ability for differentiating patients with comorbid migraine and insomnia from HC.

Our results show GMV alterations in several areas in patients with migraine relative to HC. The PCG, which is posterior to the central sulcus, is located in the parietal lobe and represents the site of the SSC, which is associated with noxious and non-noxious somatosensory processing [32]. Altered cortical thickness in the SSC, including the PCG has been reported in patients with migraine when compared with HC, which suggests a relation with structural changes of the SSC through an increased noxious afferent input [33]. Our finding of altered GMV in the PCG may, therefore, be related to repetitive migraine attacks

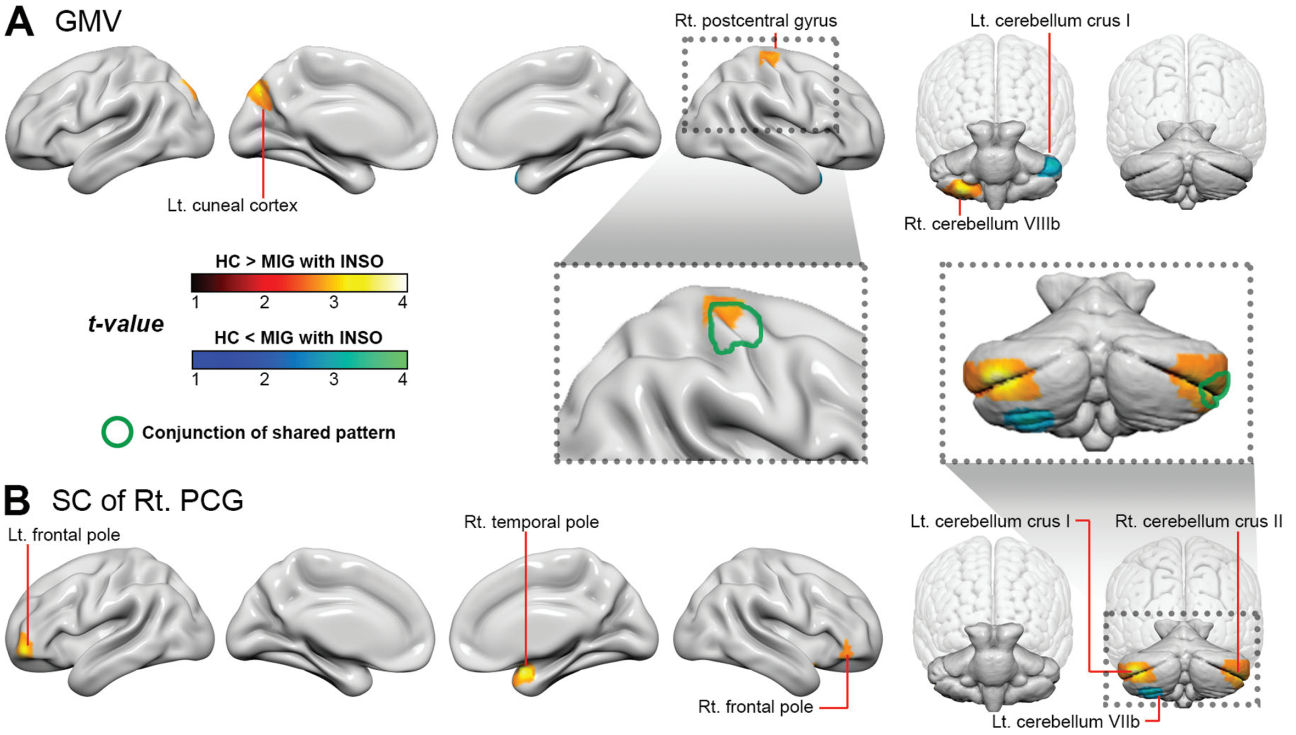

Figure 3. Differences in GMV and SC patterns of the right PCG between patients with comorbid migraine and insomnia, and HC. (A) Cold (blue) colors indicate significantly greater regional GMV in patients with comorbid migraine and insomnia; warm (red) colors indicate significantly lower regional GMV. Specifically, altered GMV was consistently found in the right PCG in patients with comorbid migraine and insomnia relative to HC (green circle). (B) Cold (blue) colors indicate significantly greater SC integrity of the right PCG in patients with comorbid migraine and insomnia; warm (red) colors indicate significantly lower SC integrity of the right PCG. Specifically, decreased integrity of structural covariance of the right PCG was consistently found in the right cerebellum in patients with comorbid migraine and insomnia, relative to HC (green circle). GMV, gray matter volume; HC, healthy controls; INSO, insomnia; Lt, left; MIG, migraine; PCG, postcentral gyrus; Rt, right; SC, structural covariance.

with neuroplastic changes in cortical structures within the trigeminal somatosensory system. Previous studies in migraineurs relative to HC have found decreases in the GMV in the precentral gyrus, which is part of the frontal motor cortex, involved in executing functions and thought to be part of the pain processing network [9]. Furthermore, the cerebellum and the deep cerebellar nuclei have been suggested to play roles in trigeminal nociception and pain modulation [34]. Therefore, our results of GMV changes in frontal precentral and cerebellar areas may be associated with interictal altered pain modulation and executive functions in patients with migraine.

Herein, patients with insomnia showed GMV decreases in the precentral and lingual gyri when compared with controls. The involvement of the precentral gyrus, which was in line with a prior study in patients with insomnia, suggests that GMV deficits of frontal precentral structures may be associated with disturbed nocturnal sleep [35]. The lingual gyrus, also known as the medial occipitotemporal gyrus, is a brain structure that is related to visual perceptual processing and emotion [36]. Altered functional connectivity (FC) in the lingual gyrus has been reported in patients with insomnia and is thought to be related to disruptions of the emotional circuit and sensory hyperarousal [37]. This suggests that the GMV changes in the lingual gyrus we observed may be related to the cognitive and affective impairments commonly experienced by patients with insomnia.

To date, only a few neuroimaging studies have investigated the shared and distinct neural properties of migraine and its comorbidities [26, 38]. A prior study observed disrupted FC predominantly affecting the sensorimotor and attention-related networks in patients with migraine with and without sleep-related movement disorder (restless legs syndrome [RLS]) [38]. Further research reported a common pattern of GMV changes predominantly affecting the middle frontal gyrus in patients with comorbid migraine and RLS [26]. Collectively, these studies suggested neuroimaging signatures related to the pathophysiology of migraine and its comorbidities, and our results are in line with this notion.

Our conjunction analysis of GMV alterations common to migraine and insomnia indicates that the GMV of the PCG is altered in both migraine and insomnia. Previous research has suggested that functional alteration of the SSC (including the PCG) is related to a dysfunction in the integration of pain sensitivity and pain processing in patients with migraine [39]. Greater thickening of the PCG in relation to increasing headache duration and frequency has been suggested to be related to increased noxious afferent input within the trigemino-thalamo-cortical pathway in migraine [33]. Furthermore, decreased GMV in primary somatosensory areas (including the PCG) in individuals with sleep deprivation may be associated with impairments of sensory-informational processing and cognitive function [40]. Collectively, these findings suggest that the comorbidity pathogenesis of migraine and insomnia may be associated with a dysfunction of sensory integration and processing and that the PCG may be involved in the comorbidity of both diseases.

To further elucidate the associated neocortical network changes of the shared GMV change regions for the comorbidity of each disorder, we used seed-based SCN analyses, followed by conjunction analyses, and thereby identified the structural

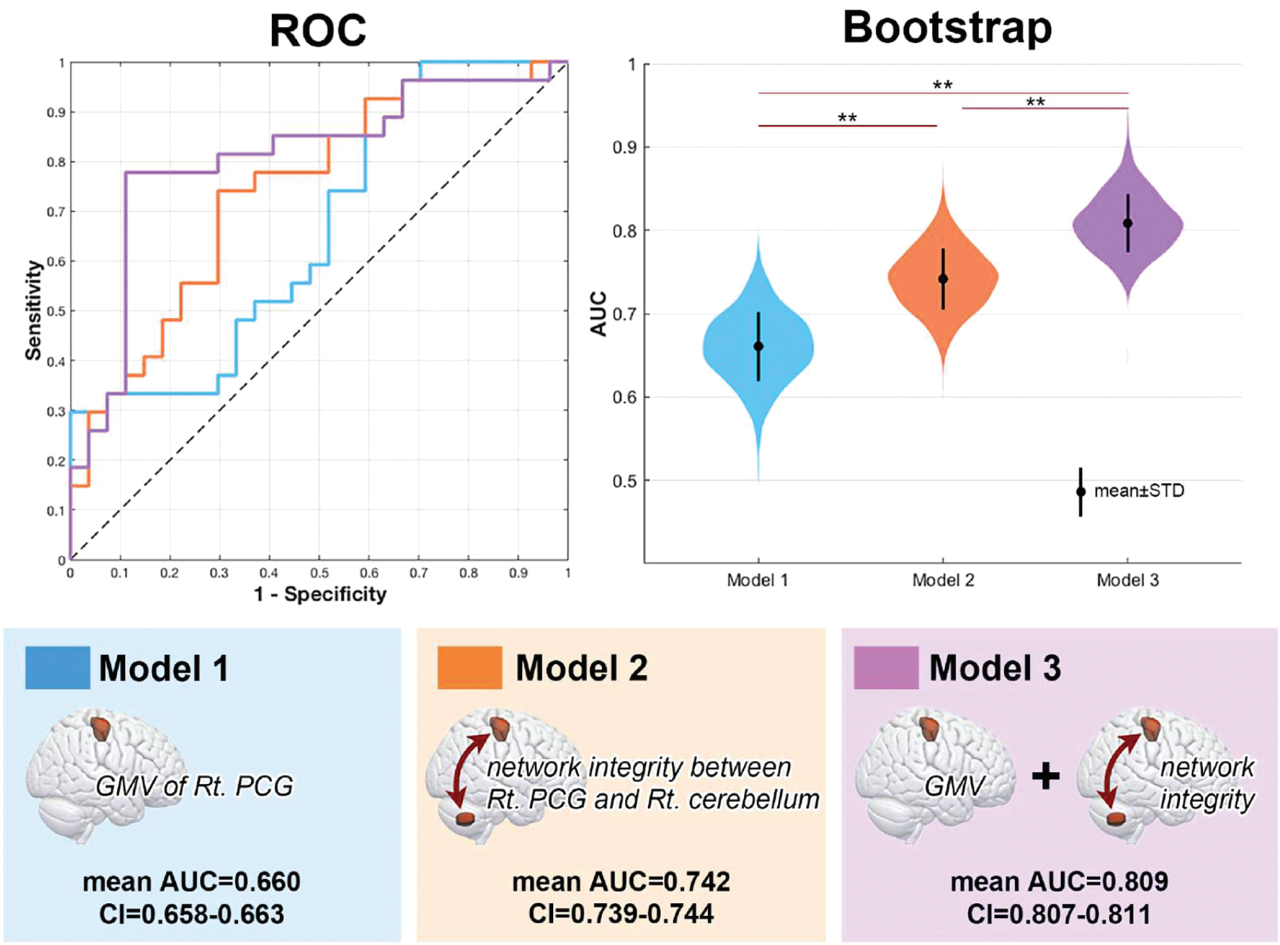

Figure 4. ROC analysis of the three distinct logistic regression models. The ROC curves (upper left panel) represent the classification performance of the three models (differentiating comorbid participants from HC): GMV of the right PCG (Model 1, blue), SC integrity between the right PCG and the right cerebellum (Model 2, orange), and the combined regional GMV and SC integrity index (Model 3, purple). The histogram shows the estimated AUC, calculated with a 1,000-times bootstrapping resampling scheme (upper right panel). AUC, area under the curve; CI, confidence interval; GMV, gray matter volume; HC, healthy controls; PCG, postcentral gyrus; ROC, receiver-operating characteristic; Rt, right; SC, structural covariance; STD, standard deviation.

covariance alterations of the PCG common to both groups, located in the cerebellum. Although the PCG and the cerebellum are, respectively, located in the SSC and the motor control area, accumulative research has demonstrated alterations in brain activity in both the PCG and the cerebellum in patients with insomnia [41]. Aberrant FC activity between the anterior insula and several sensorimotor regions, including the PCG and the cerebellum, suggests an aberrant sensory processing system in patients with insomnia [42]. Conversely, increases in cerebellar-cortical connectivity in brain regions, including the insula, during trigeminal nociception stimulation has been observed [34]. Both the PCG and insula also play important roles in the trigemino-thalamo-cortical nociceptive pathway, which has been implicated in migraine pathophysiology [43]. Furthermore, altered FC between the primary SSC (including the PCG) and the cerebellum in migraineurs has also been reported [44]. Taken together, our SCN findings that aberrant structural covariance between the PCG and the cerebellum is common to both disease groups may further suggest that the aberrant sensory processing and motor control pathway associated with the PCG, these specific vulnerable regions, may be critically involved in the pathophysiology of comorbidity of migraine and insomnia.

Our study highlights alterations in GMV and in the integrity of structural covariance of the right PCG are consistently found in patients with comorbid migraine and insomnia. Additionally, we observed a negative association with sleep quality between the GMV of the right PCG and PSQI scores in patients with comorbid migraine and insomnia, with smaller GMV of the PCG indicating poorer sleep quality. A prior study has reported that effective FC from the insula to several sensorimotor regions, including the PCG, negatively correlated with PSQI and ISI scores, suggesting aberrant salience processing functions in patients with insomnia [42]. We therefore speculate that the GMV of the PCG might be a potential biomarker for indexing sleep quality in patients with comorbid migraine and insomnia. Moreover, we also found that the combined regional GMV and integrity of structural covariance of the PCG showed better discriminative ability for distinguishing patients with comorbid migraine and insomnia from HC. This result reinforces the critical role of the regional and global characteristics of the PCG in the comorbidity pathophysiology of both disorders.

To the best of our knowledge, this study is the first to investigate regional and global neuroanatomical changes in patients with migraine or insomnia as well as those with comorbid migraine and insomnia. However, these results should be

interpreted with caution. First, we used a cross-sectional group comparison design, and the causality of the comorbidity relationship could therefore not be assessed. Future studies with longitudinal designs should be considered to determine whether these regional and global network alterations are a part of the pathogenesis or consequences of the disorders. Second, our analysis, using a strict and well-characterized diagnosis for the disease and comorbidity groups, resulted in a relatively modest sample size, which limited the generalization of our results to large disease populations. However, our exploratory findings stimulate and guide future studies including larger subject populations, which may validate or extend the current results. Finally, structural MRI (including T1-weighted images, diffusion-weighted images, and other structural image modalities) is not a direct approach to study the underlying brain anatomy, and the outcome of any derived quantitative measures could be dependent on confounding factors that contribute to the change in voxel intensity of the MRI images [45, 46]. Therefore, limited to our current case–control study design, we could not fully exclude every potential confounding factor that could be associated with MRI signal variation, and caution is needed when interpreting the observed results. In the future, advanced image acquisition, a suitable computational modeling approach, and a better study design and characterization of study participants are needed to uncover the potential underlying mechanisms of the observed T1-VBM-based tissue volume changes.

In conclusion, we identified regional and network-level neuroanatomical alterations in patients with migraine, insomnia, and comorbid migraine and insomnia. Patients with both migraine and insomnia displayed a shared regional pattern of GMV changes affecting the PCG. Furthermore, our SCN analysis of the PCG demonstrates that the anatomically distinct cerebellar region is related to the disease comorbidity. Additionally, altered GMV and integrity of structural covariance of the PCG were consistently found in patients with the comorbid condition, and the GMV of this area is also associated with sleep quality. Our findings suggest that multilevel neuroanatomical changes could be potential image markers in patients with comorbid insomnia and migraine. Our results thus provide insights into the regional and global neuroanatomical signatures related to the pathophysiology of the two common disorders.

Supplementary material

Supplementary material is available at *SLEEP* online

Acknowledgments

The authors acknowledge the MRI of Tri-Service General Hospital, National Defense Medical Center, Taiwan for their assistance with the MRI experiments.

Funding

This project was supported in part by grants from the Ministry of Science and Technology of Taiwan (MOST 107-2221-E-010-010-MY3, MOST 108-2314-B-016-023-) and from Tri-Service General Hospital, Taiwan (TSGH-C107-072, TSGH-C108-100, TSGH-D-109101).

Disclosure statement

Financial disclosure: All authors have no financial conflicts of interest to declare.

Nonfinancial disclosure: None.

References

1. Ohayon MM. Epidemiology of insomnia: what we know and what we still need to learn. *Sleep Med Rev.* 2002;**6**(2):97–111.
2. Léger D, *et al*. Daytime consequences of insomnia symptoms among outpatients in primary care practice: EQUINOX international survey. *Sleep Med*. 2010;**11**(10):999–1009.
3. Lin YK, *et al*. Associations between sleep quality and migraine frequency. *Medicine (Baltimore)*. 2016;**95**:e3554.
4. Haut SR, *et al*. Chronic disorders with episodic manifestations: focus on epilepsy and migraine. *Lancet Neurol*. 2006;**5**(2):148–157.
5. Freedom T, *et al*. Headache and sleep. *Headache*. 2013;**53**(8):1358–1366.
6. Foo H, *et al*. Brainstem modulation of pain during sleep and waking. *Sleep Med Rev.* 2003;**7**(2):145–154.
7. Holland PR. Headache and sleep: shared pathophysiological mechanisms. *Cephalalgia*. 2014;**34**(10):725–744.
8. Maleki N, *et al*. Migraine attacks the Basal Ganglia. *Mol Pain*. 2011;**7**:71.
9. Kim JH, *et al*. Regional grey matter changes in patients with migraine: a voxel-based morphometry study. *Cephalalgia*. 2008;**28**(6):598–604.
10. Riemann D, *et al*. Chronic insomnia and MRI-measured hippocampal volumes: a pilot study. *Sleep*. 2007;**30**(8):955–958.
11. Winkelman JW, *et al*. Increased rostral anterior cingulate cortex volume in chronic primary insomnia. *Sleep*. 2013;**36**(7):991–998.
12. Altena E, *et al*. Reduced orbitofrontal and parietal gray matter in chronic insomnia: a voxel-based morphometric study. *Biol Psychiatry*. 2010;**67**(2):182–185.
13. Wang L, *et al*. Altered default mode and sensorimotor network connectivity with striatal subregions in primary insomnia: a resting-state multi-band fMRI study. *Front Neurosci*. 2018;**12**:917.
14. Chong CD, *et al*. Structural co-variance patterns in migraine: a cross-sectional study exploring the role of the hippocampus. *Headache*. 2017;**57**(10):1522–1531.
15. Spreng RN, *et al*. Structural covariance reveals alterations in control and salience network integrity in chronic schizophrenia. *Cereb Cortex*. 2019;**29**(12):5269–5284.
16. Chou KH, *et al*. Structural covariance networks of striatum subdivision in patients with Parkinson's disease. *Hum Brain Mapp*. 2015;**36**(4):1567–1584.
17. Liu HY, *et al*. The cerebellum is associated with 2-year prognosis in patients with high-frequency migraine. *J Headache Pain*. 2020;**21**(1):29.
18. Olesen J. The international classification of headache disorders, 3rd edition. *Cephalagia*. 2013;**33**:629–808.
19. Regier DA, *et al*. The DSM-5: classification and criteria changes. *World Psychiatry*. 2013;**12**(2):92–98.
20. Bastien CH, *et al*. Validation of the Insomnia Severity Index as an outcome measure for insomnia research. *Sleep Med*. 2001;**2**(4):297–307.
21. Buysse DJ, *et al*. The Pittsburgh Sleep Quality Index: a new instrument for psychiatric practice and research. *Psychiatry Res*. 1989;**28**(2):193–213.

22. Beck AT, *et al*. An inventory for measuring depression. *Arch Gen Psychiatry*. 1961;**4**:561–571.
23. Zigmond AS, *et al*. The hospital anxiety and depression scale. *Acta Psychiatr Scand*. 1983;**67**(6):361–370.
24. Ashburner J, *et al*. Voxel-based morphometry–the methods. *Neuroimage*. 2000;**11**(6 Pt 1):805–821.
25. Ashburner J. A fast diffeomorphic image registration algorithm. *Neuroimage*. 2007;**38**(1):95–113.
26. Yang FC, *et al*. Patterns of gray matter alterations in migraine and restless legs syndrome. *Ann Clin Transl Neurol*. 2019;**6**(1):57–67.
27. Mechelli A, *et al*. Structural covariance in the human cortex. *J Neurosci*. 2005;**25**(36):8303–8310.
28. Bernhardt BC, *et al*. Mapping limbic network organization in temporal lobe epilepsy using morphometric correlations: insights on the relation between mesiotemporal connectivity and cortical atrophy. *Neuroimage*. 2008;**42**(2):515–524.
29. Bernhardt BC, *et al*. Selective disruption of sociocognitive structural brain networks in autism and alexithymia. *Cereb Cortex*. 2014;**24**(12):3258–3267.
30. Alexander-Bloch AF, *et al*. On testing for spatial correspondence between maps of human brain structure and function. *Neuroimage*. 2018;**178**:540–551.
31. Eisenberg IW, *et al*. Insistence on sameness relates to increased covariance of gray matter structure in autism spectrum disorder. *Mol Autism*. 2015;**36**:1567–1584.
32. Price DD, *et al*. Does the spinothalamic tract to ventroposterior lateral thalamus and somatosensory cortex have roles in both pain sensation and pain-related emotions? *J Pain*. 2002;**3**(2):105–108; discussion 113.
33. Kim JH, *et al*. Thickening of the somatosensory cortex in migraine without aura. *Cephalalgia*. 2014;**34**(14):1125–1133.
34. Mehnert J, *et al*. Activity and connectivity of the cerebellum in trigeminal nociception. *Neuroimage*. 2017;**150**:112–118.
35. Joo EY, *et al*. Brain gray matter deficits in patients with chronic primary insomnia. *Sleep*. 2013;**36**(7):999–1007.
36. Kircher TT, *et al*. Towards a functional neuroanatomy of self-processing: effects of faces and words. *Brain Res Cogn Brain Res*. 2000;**10**(1–2):133–144.
37. Kay DB, *et al*. Sleep-wake differences in relative regional cerebral metabolic rate for glucose among patients with insomnia compared with good sleepers. *Sleep*. 2016;**39**(10):1779–1794.
38. Yang FC, *et al*. Altered brain functional connectome in migraine with and without restless legs syndrome: a resting-state functional MRI study. *Front Neurol*. 2018;**9**:25.
39. Zhang J, *et al*. Increased default mode network connectivity and increased regional homogeneity in migraineurs without aura. *J Headache Pain*. 2016;**17**(1):98.
40. Dai XJ, *et al*. Plasticity and susceptibility of brain morphometry alterations to insufficient sleep. *Front Psychiatry*. 2018;**9**:266.
41. Li C, *et al*. Abnormal spontaneous regional brain activity in primary insomnia: a resting-state functional magnetic resonance imaging study. *Neuropsychiatr Dis Treat*. 2016;**12**:1371–1378.
42. Li C, *et al*. Aberrant effective connectivity of the right anterior insula in primary insomnia. *Front Neurol*. 2018;**9**:317.
43. Goadsby PJ, *et al*. Pathophysiology of migraine: a disorder of sensory processing. *Physiol Rev*. 2017;**97**(2):553–622.
44. Zhang J, *et al*. The sensorimotor network dysfunction in migraineurs without aura: a resting-state fMRI study. *J Neurol*. 2017;**264**(4):654–663.
45. Weinberger DR, *et al*. Finding the elusive psychiatric "lesion" with 21st-century neuroanatomy: a note of caution. *Am J Psychiatry*. 2016;**173**(1):27–33.
46. Lerch JP, *et al*. Studying neuroanatomy using MRI. *Nat Neurosci*. 2017;**20**(3):314–326.